Int. J. Chem. Sci.: 6(3), 2008, 1463-1479

STUDIES ON GROWTH, STRUCTURAL AND OPTICAL PROPERTIES OF LINEAR ORGANIC SINGLE CRYSTAL IMIDAZOLE

P. M. ANBARASAN*, G. MEENAKSHI[a], K. JEYAPRIYA[a], N. SAKTHIVEL and K. SUBRAMANI[b]

Department of Physics, Periyar University, SALEM - 636 011 (T. N.) INDIA
[a]Department of Physics, K. M. Centre for P.G. Studies, PUDUCHERRY - 605 008 (T. N.) INDIA
[b]Department of Chemistry, K. M. Centre for P.G. Studies, PUDUCHERRY - 605 008 (T. N.) INDIA

ABSTRACT

Single crystal of linear optical imidazole has been grown in the laboratory by using low temperature solution growth technique. The cell parameters were determined by powder X-ray diffraction analysis. FT-Raman and FT-IR analysis were used to confirm the presence of various functional groups in the grown crystal. ab initio Hartee-Fock calculations and DFT levels invoking 6-31G(d,p) and 6-311G(2df,2p) basis sets were also carried out and the results are compared with the experimental values. Thermal analysis was performed to study the thermal stability of the grown crystals. The crystals posses lower UV-cut off wavelength at 50 nm, as confirmed by the transmittance study. Kurtz powder SHG measurement confirms the non-existence of non-linear property of the grown crystal. It is suggested that the design and the synthesis of two conjugated donor-acceptor imidazole derivatives[1,2] can be carried out for second-order nonlinear optics along with Z-scan technique.

Key words: Single crystal growth, Solution growth**,** FT-IR, FT-Raman, ab initio, DFT (Density Functional Theory), DSC technique, Nonlinearlty technique.

PACS: 81.10.Dn, 42.70.Mp, 78.20.-e

INTRODUCTION

Crystal growth has been attracting the attention of large number of scientists from the academic and/or technological point of view. Considerable effort has been devoted to the study of this problem by means of various approaches. In the long history of these investigations, physicists have been mainly interested in the spontaneous pattern of formation associated with the growth of crystals[1]. In other words, why and how is these

* Author for correspondence; E-mail: anbarasanpm@gmail.com

spatially symmetric growth from the initially "Uniform" state of super cooled and/or super saturated environment phase self organized, as observed in snow flakes[2-7]. Various authors have reported much remarkable work on this topic[8-13].

Here, an attempt has been made to obtain a crude picture of one particular aspect of crystal growth. Assuming an unstable configuration of crystal growth environment, we can also show how the new and transient structure (needle) comes out from the solution growth technique. A molecular crystal suitable for the usage in a number of optically linear devices required at least four basic qualities i.e. it should possess high molecular induced polarisability, suitable crystallographic structure, sufficient crystal qualities and high thermal stability. The crystal structure shows a Centro-symmetric nature in the case of imidazole.

The present work reports the growth and characterization of an organic linear optical crystal imidazole with molecular formula $C_3H_4N_2$ as shown in the Fig. 2. The molecular structure of imidazole has got the hydroxyl group OH, which is an electron donor. Hence, the charge transfer interaction can be established, which will increase the molecular polarisability. Imidazole has got a very large transmission cut-off wavelength less than 200 nm[14]. Imidazole is incorporated into many important biological molecules. The most obvious is the amino acid histidine, which has an imidazole side chain. Histidine is present in many protein and enzymes and plays a vital part in the structure and binding functions of hemoglobin. Histidine can be decarboxylated to histamine, which is also a common biological compound. It is a component of the toxin that causes urtiaria, which is basically an allergic reaction.

The presence of impurities definitely has influence over the properties and the growth condition of the crystal; thus, enhancing the technological application of the material. It is well known that the paramagnetic fragnance (radical) can be trapped in a crystal matrix. Hence, to understand the complete physical aspects of the grown single crystal imidazole, different types of characterization analysis were made and reported here.

EXPERIMENTAL

Synthesis of laboratory grown crystal

Imidazole can be synthesized by numerous methods besides the Debus method. Many of these syntheses can also be applied to different substituted imidazoles and imidazole derivatives simply by varying the functional groups on the reactants. In literature, these methods are commonly categorized by which and how many bonds form to

make the imidazole rings. For example, the Debus method forms the (1, 2), (3, 4) and (1, 5) bonds in imidazole, using each reactant as a fragment of the ring, and thus, this method would be a three-bond-forming synthesis. In the low temperature solution growth technique, 13.43 g of glyoxal, 1.5 g of formaldehyde in 5.26 g of ammonia was dissolved in 15 mL of distilled water to form imidazole. This synthesis provides relatively low yields, but it is still used for forming C-imidazole.

Solution and solubility

The grown imidazole has been dissolved in different organic solvents like water, benzene, ethyl acetate, acetone, ethanol and methanol. It is found that water is the best suitable solvent for growing well shaped imidazole crystal. The solution of the crystal imidazole was prepared in water and maintained at 25°C with continuous stirring to ensure homogeneous temperature and concentration over the entire volume of the solution. On reaching the saturation, the content of the solution was analysed gravimetrically and this process was repeated for every 5°C. This procedure has been repeated for every temperature and a solubility curve was drawn by taking temperature along the X-axis and concentration along the Y-axis shown in Fig.1.

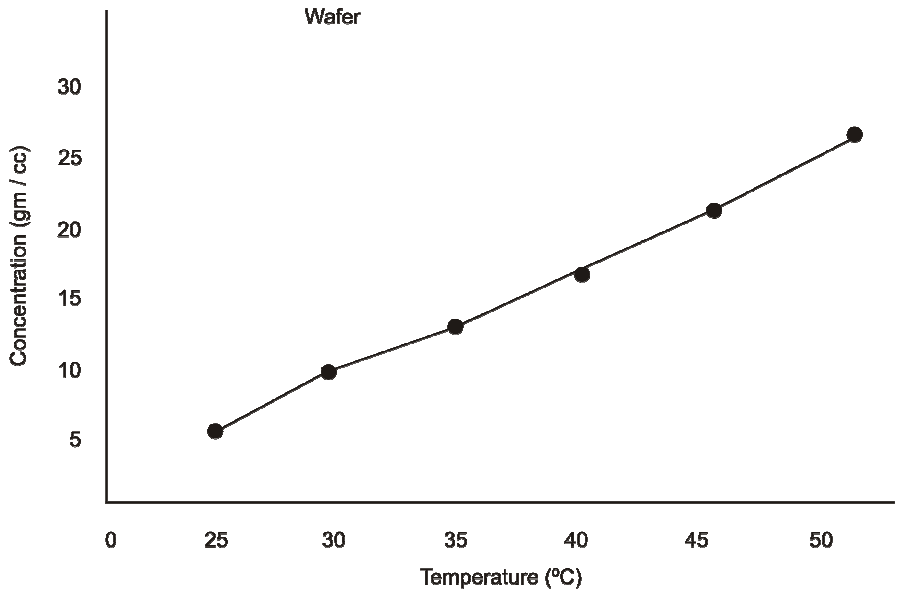

Fig. 1: Solubility curve of imidazole

The curve shows that it has a high solubility and a positive solubility temperature

gradient. From the solubility curve, a linear variation in the temperature range of 30-50°C is observed. Hence, it is concluded that 40°C will be the optimum temperature for crystal growth in water.

Growth of single crystal of imidazole

Single crystal of imidazole has been grown by solvent evaporation technique from the saturated solution. In the present work, water has been used as solvent since it was observed that when compared with other solvents, crystals grown from water were well shaped. The saturated solution was prepared from water at 40°C using a temperature controlled magnetic stirrer. The solution was kept in an optically heated constant temperature bath (with temperature setting 40°C ± 0.01°C). After repeating recrystallisation, good quality of single crystals were obtained from the other solution with dimensions (7 x 1.0 x 0.4 mm^3) approximately within a week time. Chemical strucutre (different view) and the principle crystallographic axis viz. a, b and c* were identified and are shown in Fig. 2 .

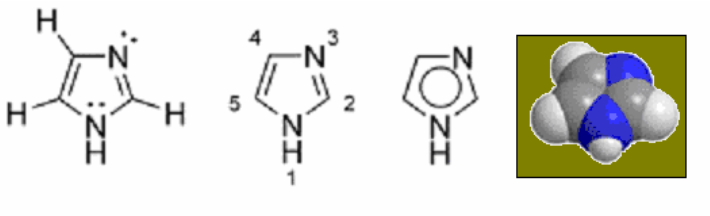

(a) **(b)** **(c)** **(d)**

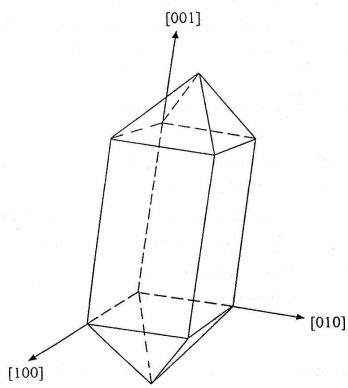

(e)

Fig. 2: Different view of chemical structure (a) to (d) and morphology diagram of imidazole (e)

The photograph of grown crystal of imidazole is shown in Fig. 3. The grown pure crystals without having any crack formation inside were characterized by following methods. Table 1 shows the prescription data for the sample imidazole.

Table 1. Prescription data for the sample imidazole

IUPAC Name	1,3-Diazole
Other names	Imidazole 1,3-Diazacyclopenta-2,4-diene
Molar mass	68.08 g/mol
Appearance	white or pale yellow solid
Density	1.23 g/cm^3, solid
Melting point	89-91 °C (362-364 K)
Boiling point	256 °C (529 K)
Acidity (pKa)	pKa = 6.993
Crystal structure	Monoclinic
Corordination geometry	Planar 5-membered ring
Dipole moment	12.8 Cm*10^{30}

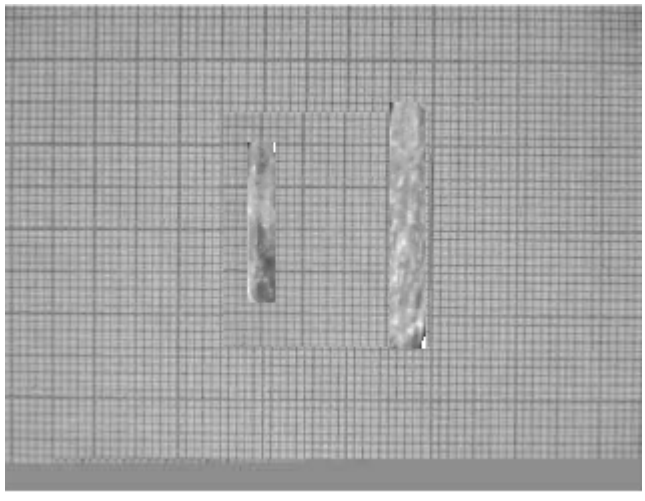

Fig. 3: Photograph of grown crystal of imidazole

Characterization

The unit cell constants of imidazole were determined using ENRAF-NONIUS CAD-4 single crystal X-ray diffractometer with *MoKα* (λ = 0.7101Å) in *ω/2θ* mode radiation to identify the structure and to estimate the lattice parameter. The crystal density was measured by floatation technique and the melting point of imidazole was found for finely powdered grown single crystal using TI-100 melting point apparatus.

The optical absorption and transmission spectra have been recorded for 2 mm thickness using UV-VIS-NIR spectrophotometer of Varian Cary Model in the range 400-2000 nm as shown in the Fig. 4 and 5.

FT-IR spectrum for imidazole was recorded on Perkin Elmer FT-IR spectrometer in the range of 4000 – 400 cm^{-1} following KBr Pellet technique at 300 K with scanning speed of 3 mm/sec. The model of spectrum is spectrum RX-I, and its resolution 4 cm^{-1} with detectors lithium tantalite. The FT-IR spectrum is shown in Fig. 6. The FT Raman spectrum of imidazole was also recorded in the region 4000-400 cm^{-1} with FRA Raman module equipped with Nd :YAG laser source operating at 10.6 μm line, with scanning speed of 30 $cm^{-1}min^{-1}$ of spectral width 20 cm^{-1}. The frequencies for all sharp bands were accurate to ± 2 cm^{-1}. The FT-Raman spectrum is shown in Fig. 7

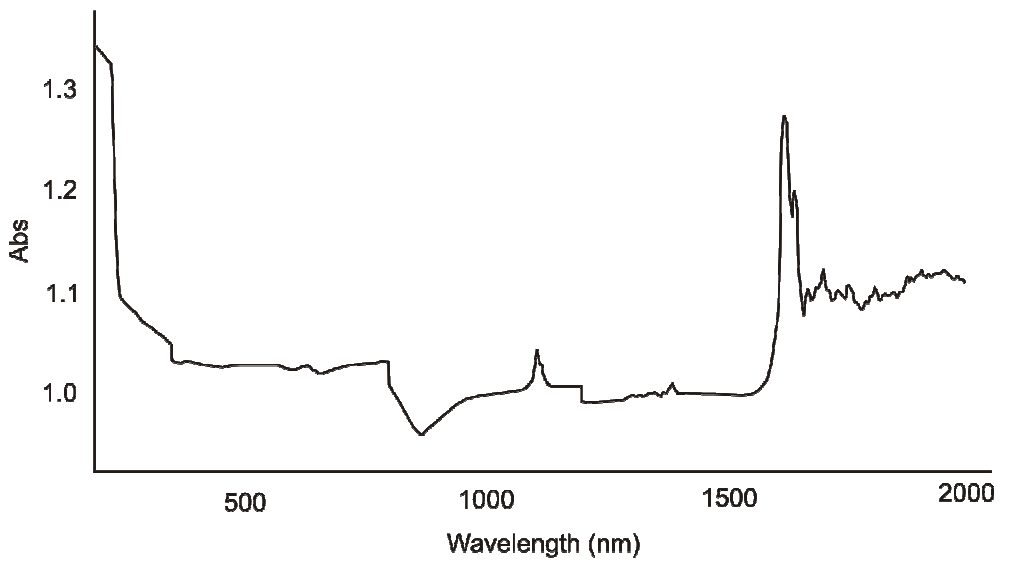

Fig. 4: UV Absorption spectrum of imidazole

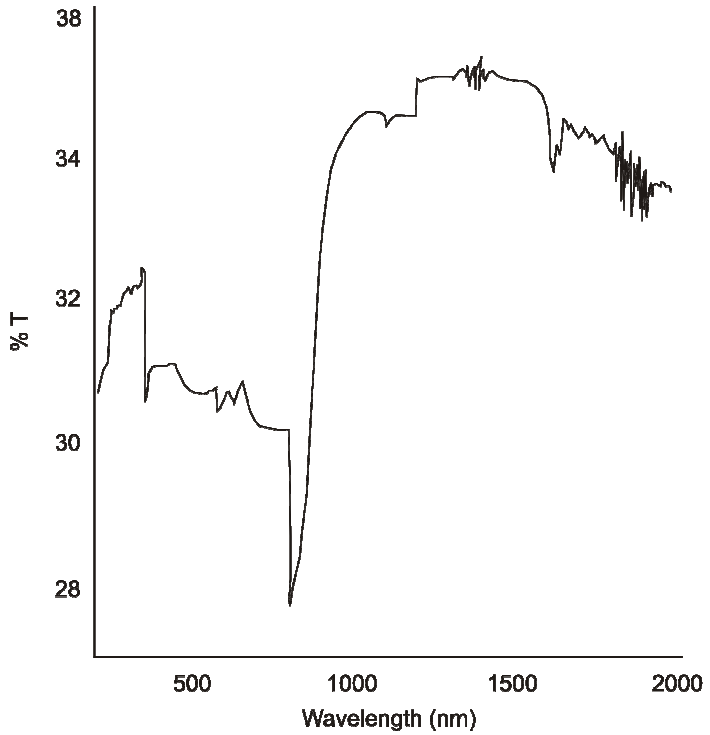

Fig. 5: UV Transmission spectrum of imidazole

The thermal analysis and hardness tests are carried out. Thermal behaviour of the crystallized complex was investigated by measuring Differential Scanning Calorimeter (DSC) thermogram (Fig. 8). The mechanical property like hardness of the crystal was studied by making indentation on (100) plane of the crystal to evaluate the Vickers's hardness number (Fig. 9).

The imidazole molecule is paired with NH_3 in order to examine the proton transfer properties of the former by ab initio methods. The primary minimum on the surface is $ImH^+\cdots NH_3$ wherein the inter-nitrogen distance in the H bond is 2.89 Å. A second well appears in the surface, corresponding to $Im\cdots{}^+HNH_3$, and the barrier between the two minima is rapidly enlarged, when the latter distance is elongated. When the NH_3 is displaced from the N lone pair direction of the imidazole in the plane of the latter, the greater proton-attracting power of the imidazole relative to NH_3 is enhanced; the opposite is observed when the NH_3 is pulled out of the imidazole plane. This distinction is explained simply on the basis of the dipole and quadrupole moments of imidazole.

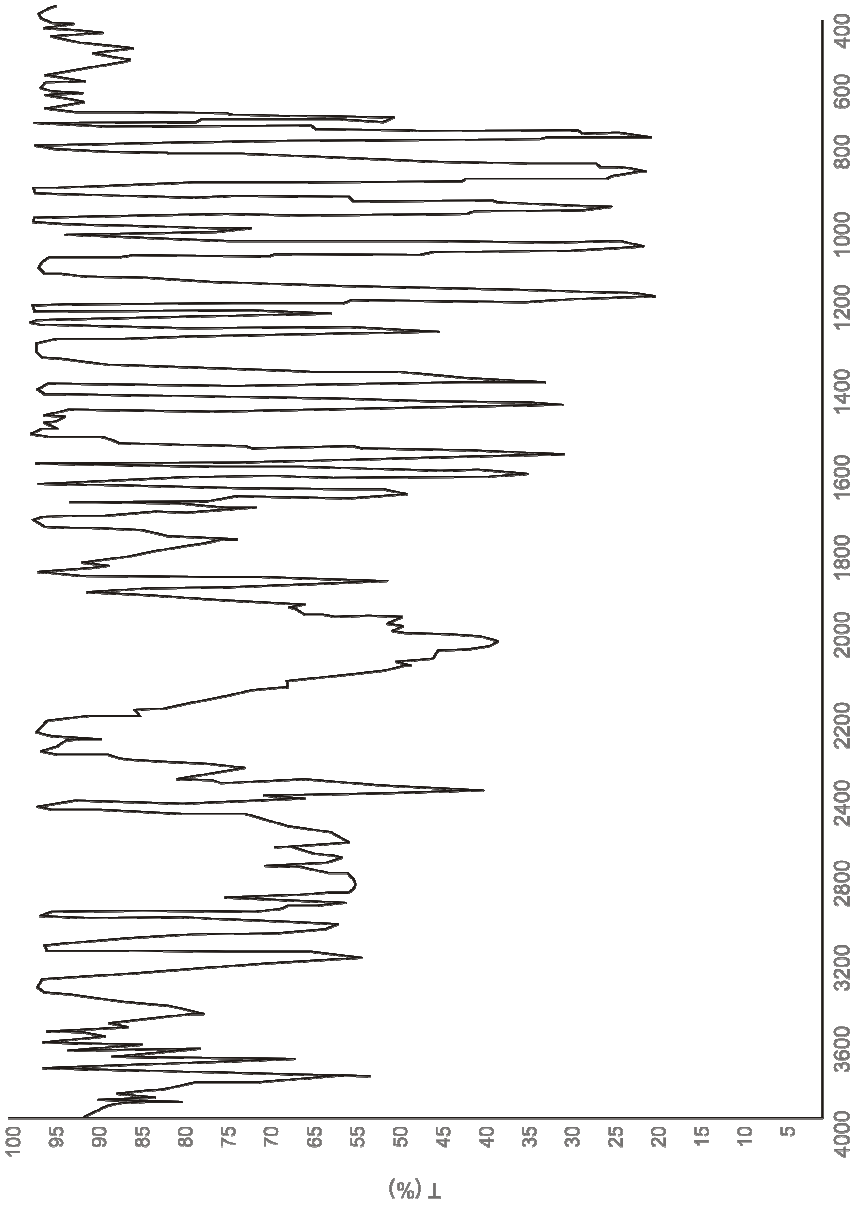

Fig. 6: FT-IR spectrum of imidazole

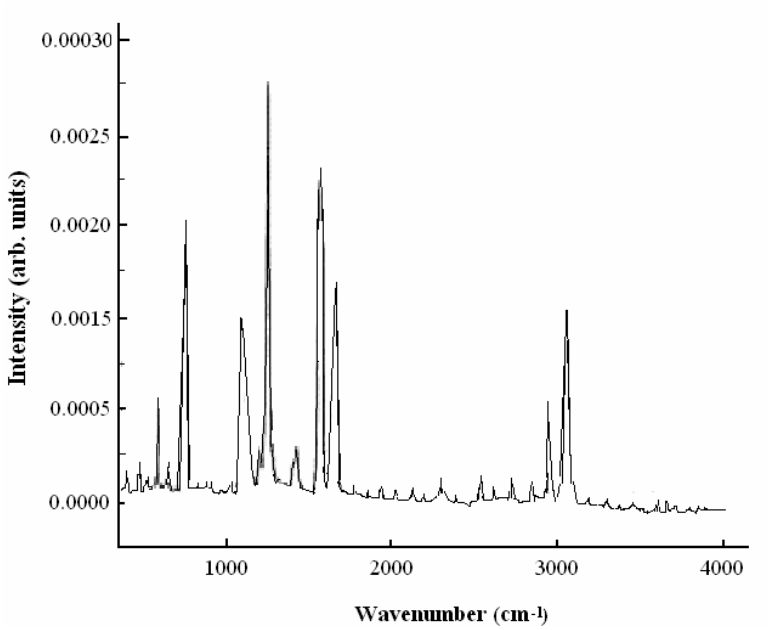

Fig.7: FT-Raman spectrum of imidazole

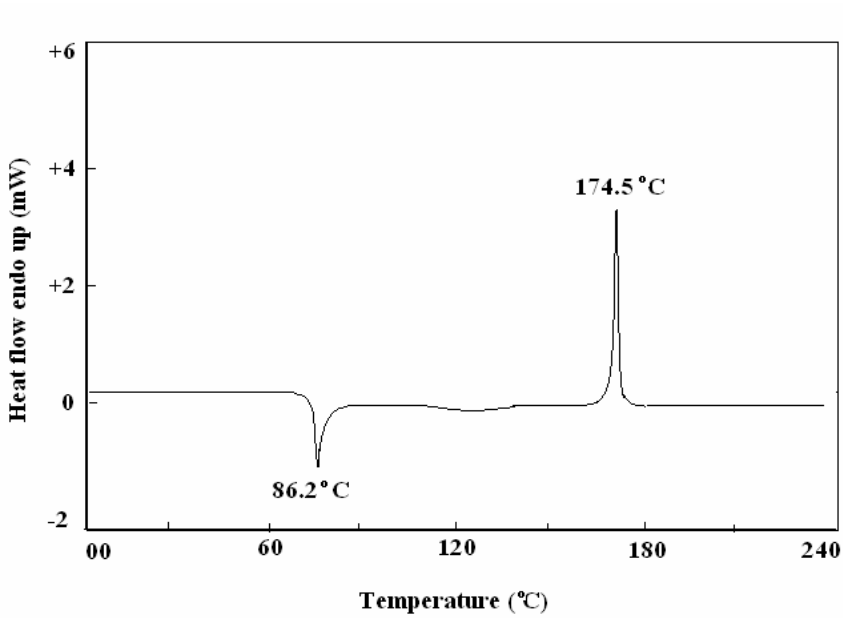

Fig. 8: DSC (Differential Scanning Calorimetry) thermogram of imidazole

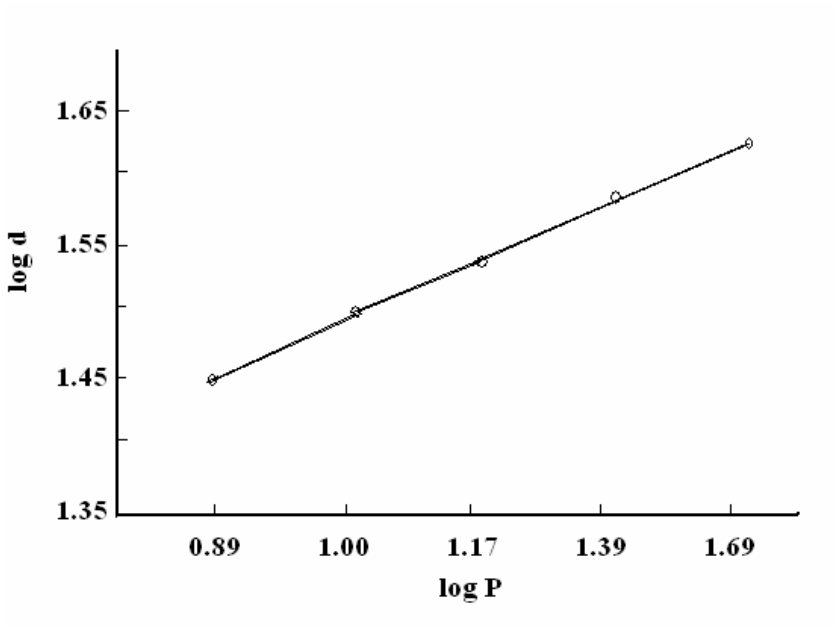

Fig. 9: Hardness graph (Plot of log P v/s log d) of imidazole

The ability of imidazole to act as a proton shuttle from one molecule to another is examined by placing one NH_3 molecule on either side. Taking $H_3NH^+\cdots ImH\cdots NH_3$ as a starting point, the simultaneous transfer of two protons to form $H_3N\cdots HIm\cdots H^+NH_3$ must overcome a large energy barrier. A stepwise process, passing through the $H_3N\cdots HImH^+\cdots NH_3$ intermediate, is greatly favored energetically. If the central imidazole is permitted the freedom to translate between the two NH_3 molecules, it is possible for the latter to be quite some distance apart. The imidazole will first approach within about 2.65 Å of the donor H_3NH^+ ion. The transfer to imidazole can then take place with little or no energy barrier. The protonated imidazole will then move close to the receptor NH_3 before depositing the proton with it. In most cases, the largest energy barrier is associated not with the proton transfers, but with the motion of the imidazole cation. The barrier for this translation grows as the ultimate donor and acceptor NH_3 molecules are moved further apart[15].

RESULTS AND DISCUSSION

X-Ray diffraction studies

The unit cell dimensions of grown imidazole were determined by single crystal X-ray diffraction technique. The system is C-face centered monoclinic with centro-

symmetric space group P21/C and cell dimensions a = 7.6806 Á, b = 5.5404 Á, c = 9.1921 Å and β = 110.8404°, which agree well with the reported values[16]. The principal crystallographic axes a, b and C* were identified and shown in Fig. 2.

Measurement of density and melting point

The measurement of density is one of the most important techniques required for the study of crystal purity. The fluctuation technique is a sensitive method to determine the density of the reference[17]. The density of imidazole was calculated theoretically using the crystallographic data as ρ = 0.6 g/cc, which agrees well with the experimental values ρ = 0.62 g/cc. A pure crystalline organic compound has in general a definite and sharp melting point i.e. the melting point range. Therefore, the melting point is a valuable criterion of purity for an organic compound. The directly measured melting point of imidazole is 89 ± 1ºC, which is in good agreement with standard value 90 - 92 ºC.

Spectral and optical study

The recorded FT-IR and FT-Raman spectra for pure imidazole crystal to show the presence of fundamental groups in the crystal lattice and the observed characteristic vibrational bands were assigned (Table 2).

Table. 2: Observed and calculated FTIR and FT-Raman frequencies (cm^{-1}) and assignments for imidazole by ab initio Hartee-Foch and density functional methods (Species A/B):

Observed frequencies (cm^{-1}) and intensity		Cal. frequency (cm^{-1})	Assignment
Laser Raman	Infrared		
3788w	3801m	3807	Hydrogen bonded stretching vibrations
3398vw	3409vw	3456	N-H asymmetric stretching vibration
3306w	3295w	3302	C-H asymmetric stretching
3108w	3111w	3109	N-H symmetric stretching
3061s	3048m	3052	-C-H symmetric stretching
2997vw	2989w	2969	N-H out-of plane bending

Cont…

Observed frequencies (cm^{-1}) and intensity		Cal. frequency (cm^{-1})	Assignment
Laser Raman	**Infrared**		
2904vw	2897w	2919	C-H stretching superimposed with N-H stretching
2871vw	2790w	2861	N- H group stretching vibrations
2699vw	2777w	2755	Strongly bonded hydrogen vibrations
2701vw	2615w	2611	N-H deformation combination bands
2388m	2381vs	2398	Overtones and combinations
2933w	2055m	2061	Double bonded stretching vibrations
2007w	2015s	1995	N-H stretching group vibrations
1799w	18048w	1871	=C-H out of plane bending
1701w	1698w	1709	C=N symmetric stretching
1678w	1683w	1666	C=C asymmetric stretching
1609s	1614s	1602	N-H torsion
1576m	1590s	1589	C=C asymmetric ring stretching
1517vw	1510vw	1508	C=C symmetric stretching
1449m	1466s	1459	C-N asymmetric stretching
1413m	1396s	1403	C-H in-plane bending
1387w	1392s	1368	C-N symmetric stretching
1249vw	1265w	1259	C-N-H stretching
1198vs	1212s	1202	N-H in-plane bending
1098s	1092s	1085	N-H twist
998m	987vs	1005	C-H in plane bending
989vw	976vw	953	C=C torsional
896s	910s	905	C-H out of plane bending
865vs	873vs	877	N-H out-of plane bending

Cont…

Observed frequencies (cm^{-1}) and intensity		Cal. frequency (cm^{-1})	Assignment
Laser Raman	**Infrared**		
856vw	877vw	854	C-H deformation
793vw	789vw	800	N-H wagging
713vs	721vs	715	C-H out of plane deformation
629w	631m	620	C=C out of plane bending
578w	563w	551	C-N out-of plane bending
439vw	462vw	453	N-H torsional oscillation

vs – Very strong s – Strong m – Medium w – Weak vw – Very Weak

In order to obtain a more complete interpretation of the vibrational spectrum and to determine the degree of normal modes, by combining the results of the GAUSSVIEW program with symmetry considerations, along with available related data, vibrations frequency assignments were made with high degree of accuracy. FT-Raman and FT-IR analysis was used to confirm the presence of various functional groups in the grown crystal. We have also carried out ab initio Hartee-Fock calculations and DFT levels invoking 6-31G(d,p) and 6-311G(2df,2p) basis sets and the results are compared with the experimental values[18].

C=C vibrations

The C=C vibrations are observed as the bands at 1683, 1590, 1510, 976 and 631cm^{-1} and 1678, 1576, 1517, 989, 629 cm^{-1} in FTIR and FT-Raman spectra, respectively. The C=C stretch can readily be assigned to the medium band in the Raman spectrum at 1576 cm^{-1}. The FTIR counter part for this mode has been identified at 1590 cm^{-1}. Three other skeletal modes containing significant contributions of C=C stretching are also assigned to the bands at 1130, and 1001 in FTIR, 943 and 925 cm^{-1} are observed in the Raman spectrum, respectively. The calculated values using with GAUSSVIEW program for C=C vibrations are 1666, 1589, 1508, 953 and 620 cm^{-1}.

C-N vibrations, C=N vibrations

The identification of the C-N stretching frequency in the imidazole is a rather difficult task since there are problems in identifying these frequencies from other

vibrations. FTIR spectrum indicates the C-N stretching band at 1466, 1392, 1265 (C-N-H) and 563 cm^{-1} in imidazole, while the stretching frequency of the C=N bond at 1701 cm^{-1} was observed in FT Raman counter part for this mode. The bands at 1449, 1387, 1249 and 578 cm^{-1} are present corresponding to C = N and C-N stretching, respectively. The calculated values of C = N vibrations are 1709, 1459, 1368, 1259 and 551 cm^{-1}.

C-H vibrations

C-H vibrations in the region 3043—3078 cm^{-1} are in agreement with experimental assignments 3040-3106 cm^{-1}. The C-H in plane bending vibrations are assigned in the region 1403-1005 cm^{-1} while the experimental observations are at 3306, 3061, 1413, 998, 896, 856 and 713 cm^{-1} and at 3295, 3048, 2898, 1396, 987, 910, 877 and 721 cm^{-1} in FTIR and FT-Raman spectra, respectively. The calculated frequencies of C-H vibrations are 3302, 3052, 2919, 1403, 1005, 905, 854 and 715 cm^{-1}.

N-H vibrations

There are twelve bands, which are identified for the N-H vibrations for imidazole in the FTIR spectrum. These are assigned to the band at 3409. 3111, 2989, 2790, 2615, 2015, 1614, 1212, 1092, 873, 787 and 462 cm^{-1} and in the FT-Raman spectrum these are observed at 3398, 3108, 2997, 2871, 2701, 2007, 1609, 1190, 1098, 865, 793 and 439 cm^{-1}. The N-H in-plane bending and N-H out-of plane bending are calculated at 1202 cm^{-1} and 715 cm^{-1}, which agree well with literature value (Sundaraganesan et al[18]).

Kurt SHG test was performed to find the non-linear optical property of imidazole. The measurement confirmed the non-existence of non-linear property of the grown crystal. The SHG of grown imidazole single crystal sample was not observed by subjecting the grown imidazole crystal to Spectra – Physics Quanta-Ray DHS2 Q-switched Nd:YAG laser radiation emitting a fundamental wavelength of 1064 nm with pulse width of 10 ns.

The transmittance maximum (peak) followed by a postfocal transmittance minimum (valley). In Z-scan technique, a polarized Gaussian laser beam propagating in the Z-direction, is focused to a narrow waist. The sample is moved along the Z-direction and the transmitted intensity is measured through a finite aperture in the far field as a function of the sample position Z, measured with respect to the focal plane. In this condition, the measured transmittance remains constant (i.e, Z-independent).

It is also suggested that the design and the synthesis of two conjugated donor-acceptor imidazole derivatives (1, 2) can be carried out for second-order nonlinear optics.

The thermal properties, the transparency and second-order nonlinear optical properties of the molecules are investigated and the experimental results indicate a good third order nonlinearity for 632 nm using He-Ne laser in P3DDT obtained by open and closed aperture Z-scan technique. Analysis of the intensity versus sample position Z-scan curve, predicated on a local response, gives the real and imaginary parts of the third order susceptibility. In this technique, the optical effects can be measured by translating a sample in and out of the focal region of an incident laser beam.

From Fig. 6 and 7 of optical absorption and transmission spectra, it is observed that the cut off wavelength is found to be 50 nm that is comparable with the earlier values.[14]

Thermal analysis

The heat capacity at constant pressure *Cp* of grown imidazole single crystal was measured by DSC analysis in the temperature range (30°C/10.00(K/min)/ 400°C). This method reveals a sharp endothermic peak at 86.2°C and an exothermic peak at 174.5°C. The endothermic transient to be attributed to the presence of un-coordinated alcohol group in this structure, since the alcoholic group is known to exhibit melting point between 89 - 91°C. The exothermic peak could be attributed to the decomposition of the substance imidazole. To calibrate the system within 2%, indium specimens were used. Powdered samples of imidazole with purity of 99.99% determined by vapour phase chromatography were placed in a sealed aluminium differential scanning calorimetric pan. The DSC curve of imidazole is shown in Fig. 8. The specific heat of imidazole at 298 K was found to be 2.754Jg $^{-1}$K $^{-1}$.

Hardness

The Vicker's hardness value was measured using the formula, and the value is found to be 85 kg/mm^3.

$$V.H.N = \left(\frac{P}{A}\right) = \left(\frac{2P\sin\frac{\theta}{2}}{d^2}\right) = 1.8544\,\frac{P}{d^2}\,Kg/mm^2 \qquad \ldots(1)$$

Fig. 9 shows the load versus Vickers's hardness number for imidazole crystal. At lower load, it is observed that the increase of load increases the hardness. This is due to the work hardening of the surface layers. Beyond the load of 50 g, a significant crack will occur. This may be due to the release of internal stress generated by indentation. Using

this study, the nature of the substance (harder or softer) can be identified.

CONCLUSION

The imidazole crystal has a very large transmission range, which will be useful for wide application, like, obtaining Raman coherence source spectroscopic real time analysis holography, ultra high speed optical gate amplifiers, Choppers etc. The crystal structure is stabilized by hydrogen bonding. We have carried out ab initio and density functional theory calculation on the structure and vibrational spectrum of imidazole. Comparison between the calculated and experimental structural parameters indicates that B3LYP are in good agreement with experimental ones. Vibrational frequencies, infrared intensities and Raman activities calculated by B3LYP/6-311G(2df,2p) method agree very well with experimental results. This study demonstrates that scaled DFT/B3LYP calculations are powerful approach for understanding the vibrational spectra of organic single crystal imidazole. Optical properties, such as second and third harmonic order generation techniques were carried out to check the nonlinearity of the imidazole crystal.

The elucidation of molecular structure from FT-IR and FT-Raman studies confirmed the purification of the crystal. The growth rate is high along C-axis. The thermal behaviour of imidazole studied by DSC supported the structure suggested.

ACKNOWLEDGMENT

The authors are thankful to Dr. Palani Balaya, Faculty of Engineering, National University of Singapore, Singapore, for his continuous encouragement. The authors are also thankful to Dr. S. Moorthy Babu, Crystal Growth Centre, Anna University, Chennai-25 and Dr. N. Sundaraganesan, Department of Physics (Engg.), Annamalai University, Annamalai Nagar – 608 002, India, for the use of Laboratory and software facilities, respectively. The authors are also deeply indebted to the anonymous reviewers for their constructive and helpful comments.

REFERENCES

1. J. S. Langer, Rev. Modern Physics, **52** (1980).
2. U. Nakaya, Snow Crystals, Harvard University Press, (1954).
3. P. V. Hobbs, Ice Physics, Clarendon, Oxford, (1974) Ch. 8.
4. T. Kobayashi, Phil. Mag. **6,** 1363 (1961).

5. J. Hallett and B. J. Mason, Proc. Roy. Sec. (London) A, **247,** 440 (1958).
6. T. Kuroda, Kinetik des Eiswaschstums aus der Gasphase Und seine Wachstumsformation, Thesis, TV Braunschweig (1979).
7. T. Kuroda, J. Crystal Growth **56,** 189 (1982).
8. J. S. Langer and H. Muller-Krumbhaar, Acta Met. **26,** 1681 (1978).
9. J. S. Langer and H. Muller-Krumbhaar, Acta Met. **26,** 1689 (1978).
10. J. S. Langer and H. Muller-Krumbhaar, Acta Met. **26,** 1697 (1978).
11. W. Lodfield, Mater. Sci. Eng. **11,** 211 (1973).
12. E. G. Holtzmann, J. Appl. Phys. **41,** 1460 (1970).
13. E. G. Holtzman, J. Appl. Phys. **41,** 4769 (1970).
14. S. Dhanuskodi and S. Manikandan, Ferroelectrics **234,** 183 (1999).
15. Steve Scheiner and Manyiu Yi, J. Phys. Chem., **100,** 9835 (1996).
16. Li. Zhengdong, Su Geno, and Wu Baichang, J. Crystal Growth, **121,** 516 (1992).
17. A. F. Loffe, Phys. Stat. Sol. **116,** 457 (1989).
18. N. Sundaraganesan, B. Dominic Joshua and K. Settu, Spectrochimica Acta Part A, **66,** 381 (2007).

Accepted : 27.05.2008